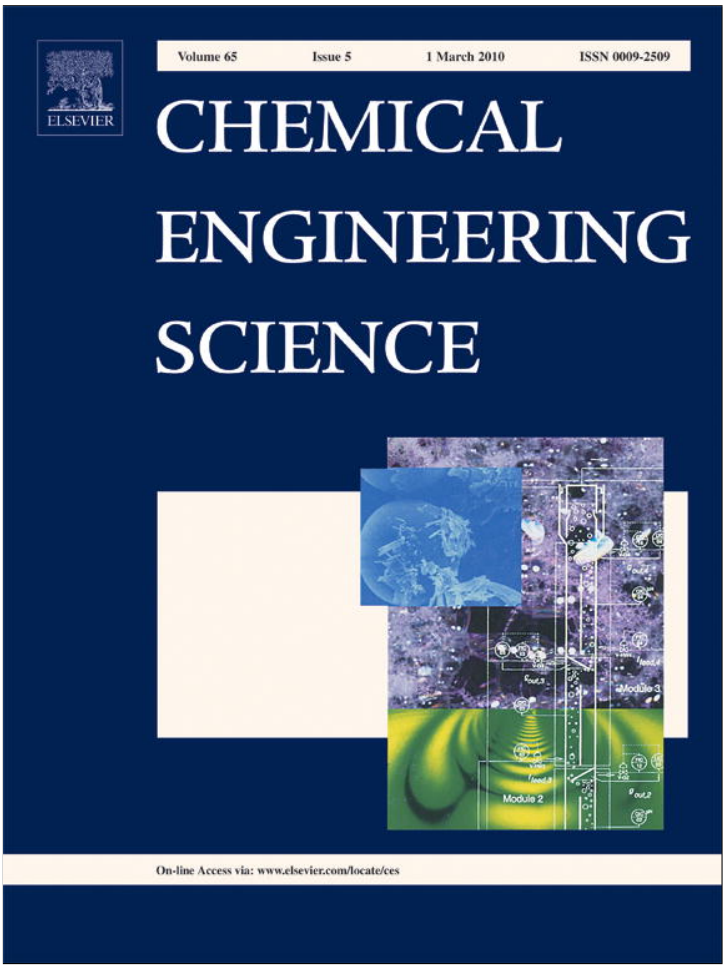

Chemical Engineering Science 65 (2010) 1563–1570

Contents lists available at ScienceDirect

Chemical Engineering Science

journal homepage: www.elsevier.com/locate/ces

Effect of surface properties on the flow characteristics and mass transfer performance in microchannels

Yuchao Zhao, Yuanhai Su, Guangwen Chen *, Quan Yuan

Dalian National Laboratory for Clean Energy, Dalian Institute of Chemical Physics, Chinese Academy of Sciences, Dalian 116023, China

ARTICLE INFO

Article history:
Received 19 October 2008
Received in revised form
10 October 2009
Accepted 24 October 2009
Available online 5 November 2009

Keywords:
Immiscible fluids
Microreactor
Microchannel
Mass transfer
Surface modification

ABSTRACT

In this work, the influence of surface properties on the flow characteristics and mass transfer performance of two immiscible liquids are investigated in the opposed and cross-flow configuration microchannels, as the volumetric flux ratio is far <1. For visually identifying flow patterns in transparent PMMA microchannels, dyed de-ionized water and kerosene are selected as test fluids. To investigate the mass transfer characteristics in stainless steel microchannels, water–succinic acid–*n*-butanol is chosen as a typical system. Reynolds number varied between 11 and 275. Only at low Re_M numbers, the dispersed phase flow pattern can occur in the opposed T-shaped PMMA microchannel before surface modification. At higher Re_M numbers, only the continuous phase flow pattern (parallel flow) is observed before and after surface modification. Moreover, the fluctuation amplitude after surface modification is larger than before surface modification at the opposed T-junction. To eliminate the effects of the sampling intervals and separation process of oil–water two phases on mass transfer performance, one new testing method is established by manufacturing the novel oil–water separator based on the principle of siphon. For the conditions applied during the study, the overall volumetric mean mass transfer coefficients range from 0.19 to 11.96 s^{-1}, which are one or three orders of magnitude higher than those in typical conventional large scaled contactors.

1. Introduction

The miniaturization of chemical processes using chip-based microchannel reactors can exhibit significant advantages over existing conventional reactors techniques, and its importance in chemical engineering, chemistry and biotechnology has increased significantly within the last decade (Ehrfeld et al., 2000; Jensen, 2001; Jähnisch et al., 2004; Chen et al., 2004; Hu et al., 2005; Cao et al., 2006). The extremely large surface-to-volume ratio and the short transport path in microchannels enhance heat and mass transfer dramatically, and hence provide many potential opportunities in chemical process development, high efficiency utilization of energy and process intensification (Mala et al., 1997; Tunc and Bayazitoglu, 2002; Kashid et al., 2007). To realize potentials of this new and promising technology, a fundamental understanding of transport processes in microchannels is necessary (Kockmann, 2007).

Although the flow of immiscible fluids in microchannels has attracted significant attention recently (Thorsen et al., 2001; Dreyfus et al., 2003; Squires and Quake, 2005), very little work seems to have been done on mass transfer of immiscible fluids (Kashid et al., 2005; Zhao et al., 2007; Dessimoz et al., 2008). Mass transfer in multiphase microfluidics, especially two immiscible phases, through microchannels is of interest when considering alternatives for process intensification (Burns and Ramshaw, 2002). Liquid–liquid two-phase flow patterns are formed when two immiscible fluids are brought in contact at the T-junction in the microchannels. There are two kinds of flow regimes. The first is both phases continuous, that is, the continuous-phase flow pattern, mainly including parallel flows with smooth or wavy interface at the T-junction, parallel flow and annular flow in the microchannel. When continuous phase and dispersed phase coexist, that is called the dispersed phase flow pattern, mainly including slugs, monodispersed droplets and chaotic thin striations formed at the junction, drop populations formed in the center of microchannel (Zhao et al., 2006).

The dispersion of one liquid into another is important in many industrial operations. When mass transfer between two immiscible liquids has to be increased, the main way in conventional chemical systems is to increase the dispersion of one liquid by increasing stirring speed, that is, to convert into smaller droplets. Similarly, some investigators testified that mass transfer of liquid–liquid two-phase system can be intensified through internal circulation in the liquid slugs (Burns and Ramshaw, 2001; Dummann et al., 2003; Kashid et al., 2005). In fact, the fundamental principle of enhancing mass transfer in microchannels

* Corresponding author. Tel.: +86 411 84379031; fax: +86 411 84379327.
E-mail address: gwchen@dicp.ac.cn (G. Chen).

0009-2509/$ - see front matter © 2009 Elsevier Ltd. All rights reserved.
doi:10.1016/j.ces.2009.10.027

is to increase the interfacial area of two phases or decrease the diffusion distance and enhance surface renewal velocity, moreover, these factors are closely linked to liquid–liquid two-phase flow patterns. It had generally been accepted that the hydrodynamics of liquid–liquid two-phase flow in microchannels were not very well understood, especially those involving multiphase fast reactions limited by mass transfer (Kashid et al., 2005). Thorsen et al. (2001) demonstrated that microfluidic devices could be used to create controllable droplet emulsions in two immiscible fluids, by injection water into a stream of oil at a T-junction. Guillot and Colin (2005) had determined the stability of parallel flows in a microchannel after a T-junction with confocal fluorescence microscopy and identified three typical flow patterns, i.e. droplets formed at the T-junction, parallel flows, parallel flows which break into droplets inside the channel. Although many investigations have been carried out in glass (Zhao et al., 2002), PMMA (Zhao et al., 2006) and PDMS (Thorsen et al., 2001; Guillot and Colin, 2005; van der Linden et al., 2006) microchannels, no much work for controlling the liquid–liquid two-phase flow patterns in stainless steel microchannels has been reported. This is unfortunate, as stainless steel is used widely in laboratory or industry because it is a kind of cheap material for the realization of microfluidic structures and has excellent chemical corrosive- and pressure-resistant capacity.

In the present investigation, the main objective is to quantitatively study the influence of surface properties on the flow characteristics and mass transfer performance of two immiscible liquids in well-defined T-junction microchannel systems at different operating conditions. Dyed de-ionized water and kerosene are selected as test fluids for visually identifying flow patterns of liquid–liquid two phases in transparent PMMA microchannels before and after surface modification. To accurately measure the overall volumetric mass transfer coefficients in the single microchannels, the new testing technology and method are established by manufacturing the novel oil–water separator based on the principle of siphon. Water–succinic acid–*n*-butanol is chosen as a typical example for investigating the mass transfer characteristics of immiscible two-phase fluids in stainless steel microchannels before and after surface modification.

2. Experimental section

2.1. Material and apparatus

The essential features of the T-junction microchannel are shown in Fig. 1(a). The T-junction microchannel formed by two channel sections joined at a right angle is the simplest microdevice for mixing two fluid streams. Two opposing streams enter coaxially from the two inlet arms and leave through the mixing channel which is perpendicular to the entering direction after colliding at the T-junction. This configuration is called the opposed T-shaped configuration micromixer as shown in Fig. 1(b). One stream passes straight through the mixing channel and the other enters through the side microchannel and collide the first stream perpendicularly. This configuration is called the cross-flow T-shaped configuration micromixer and is shown in Fig. 1(c). Table 1 shows the actual dimensions of the two kinds of T-shaped micromixers.

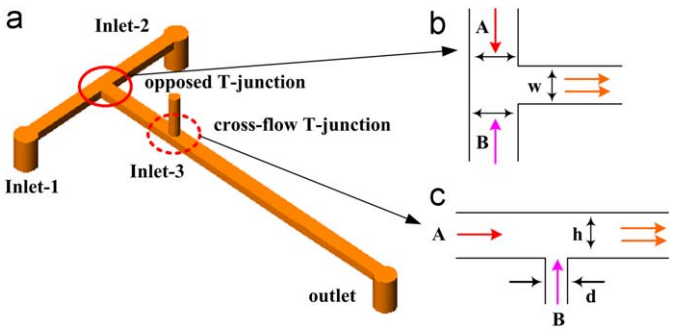

Fig. 1. (a) Schematic of the T-junction rectangular microchannel. (b) Opposed T-shaped configuration, inlet-1 and inlet-2 as the inlets. (c) Cross-flow T-shaped configuration, inlet-1 and inlet-3 as the inlets.

Table 1
Dimensions of T-junction micromixers (μm).

	Inlet-1 arm		Inlet-2 arm		Mixing channel		Inlet-3 arm
	w	*h*	*w*	*h*	*w*	*h*	*d*
Opposed	600	300	600	300	600	300	Naught
Cross-flow	600	300	Naught		600	300	500

Table 2
Physical properties of water and kerosene (at 293 K and atmospheric pressure).

Fluid	Density (kg/m^3)	Viscosity (Pa·s)
Water	998.2	0.001
Kerosene	780	0.00115

Interfacial tension σ=0.045 N/m.

The T-shaped microchannels are fabricated in the stainless steel and PMMA plate using micromachining technology (FANUC KPC-30a) in our CNC Machining Center. The surface roughness caused by micromachining process, which is in the order of several microns, is negligible compared to the characteristic scale for the microchannels in this study.

The working fluids for the investigation of flow patterns are kerosene and de-ionized water with minute amounts of methylene blue dissolved in it for better visualization of the flow phenomena in the transparent PMMA microchannels. The physical properties of water and kerosene are listed in Table 2. The flow patterns are identified using a digital video camera that is connected to a personal computer and provides snapshots. A high-speed camera system (UC-610CL) with recording speed of 61 frames per second and shutting speed of 1/110–1/110,000 s was mounted together with microscope.

The mass transfer system is chosen according to the standard test system recommended by the European Federation of Chemical Engineering (EFCE), water–succinic acid–*n*-butanol, as a typical example of liquid–liquid two-phase extraction process (Misek et al., 1985). The mass transfer experiments are carried out in stainless steel T-shaped microchannels due to the swelling effect of *n*-butanol on PMMA material.

The de-ionized water is used in all the experiments, which is first boiled in a beaker to remove the dissolved gases and fully degassed. Succinic acid and *n*-butanol are of analytical grade. The organic (*n*-butanol) phase is always saturated with aqueous phase (water) to prevent multi-component diffusion between the two phases and vice versa, so succinic acid can be considered as the only diffusing species in the mass transfer system. In the present case, the concentration of succinic acid in the aqueous phase is very low ($<1\%$), therefore, it is reasonable to assume that the properties of the two immiscible phases are constant in all experimental processes. The present paper presents our experimental method and the results from extraction experiments, as well as the mass transfer coefficients calculated using the results.

The physical properties of water–succinic acid–*n*-butanol system are listed in Table 3.

2.2. Experimental setup

The schematic diagram of the experimental apparatus is shown in Fig. 2. To maintain continuous flow without pulsation, buffer tank between the piston pump (Beijing Satellite Manufacturing Factory) and check valve is used. The aqueous and organic phases are forced to flow through the horizontal rectangular section microchannel by these high precision piston pumps, respectively.

2.3. Method and facility to analyze mass transfer

In this paper, the oil/water phase separation is very difficult using the conventional funneled separator after collecting samples from the outlet streams because the volumetric flux ratio of aqueous phase and oil phase ($q=Q_w/Q_o$) is greatly <1. To solve this problem and increase the precision for measuring mass transfer processes, a novel oil/water separator is designed and manufactured based on the principle of siphon, as shown in Fig. 3. In experimental process, the aqueous phase is siphoned into the capillary and keeps suitable height, that is, the siphon is mainly used to collect aqueous phase and separate oil–water two phases.

In all experimental runs, the capillary of the bottom of separator is close by a rubber cap and the outlet streams of T-junction microchannel enter into the separator from the top entrance, simultaneously, the aqueous phase is gone down into the capillary. Subsequently, the aqueous phase is quickly take out using a syringe after collecting samples (enough amounts for analyzing) and the amount of succinic acid transferred from the aqueous phase into the organic phase is analyzed by titration, using a standard sodium hydroxide solution as the titrant for succinic acid samples. The results show that the effect of the sampling time on mass transfer performance can be ignored, so the influence of the fifth mass transfer zone in the separator on the entire process is eliminated. The accuracy of the analytical method is tested by using known samples of aqueous solutions, and the maximum error does not exceed $\pm 3\%$.

Table 3
Physical properties of water–succinic acid–*n*-butanol system.

Mass transfer system	Density (kg/m^3)	Viscosity (Pa·s)
Saturated deionized water with *n*-butanol	981.69	0.00144
Saturated *n*-butanol with deionized water	837.01	0.00334

At 295 K and atmospheric pressure.

2.4. Determination of mass transfer coefficients

From our previous experimental results about flow patterns and mass transfer performance (Zhao et al., 2006, 2007), we know that the main mass transfer contribution is at the T-junction zone, so the pseudo-homogeneous model fluid model is chosen. The Reynolds numbers of the two immiscible phases can be calculated by the following equations:

$$Re_M = \frac{D_H U_M \rho_M}{\mu_M} \tag{1}$$

$$D_H = \frac{4A}{2(h+w)} \tag{2}$$

$$U_M = \frac{Q_{aq}+Q_{or}}{A} \tag{3}$$

$$\rho_M = \left(\frac{\varphi_{or}}{\rho_{or}} + \frac{1-\varphi_{or}}{\rho_{aq}}\right)^{-1} \tag{4}$$

$$\mu_M = \left(\frac{\varphi_{or}}{\mu_{or}} + \frac{1-\varphi_{or}}{\mu_{aq}}\right)^{-1} \tag{5}$$

$$\varphi_{or} = \frac{Q_{or}}{Q_{aq}+Q_{or}} \tag{6}$$

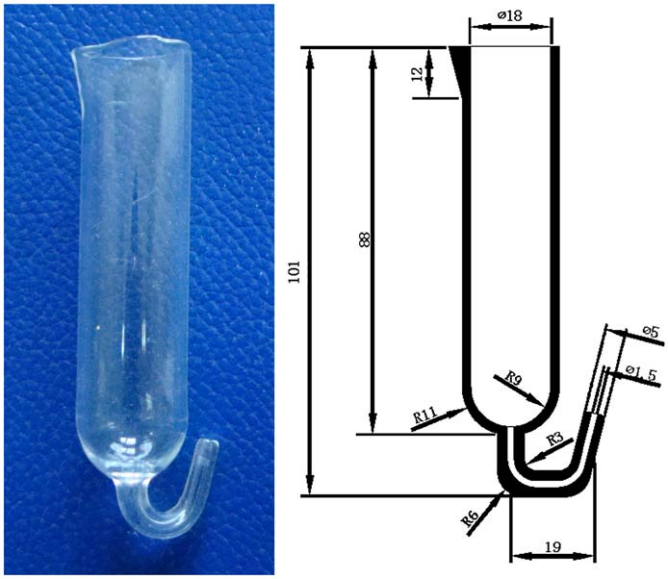

Fig. 3. Oil/water separator of home-made based on the principle of siphon.

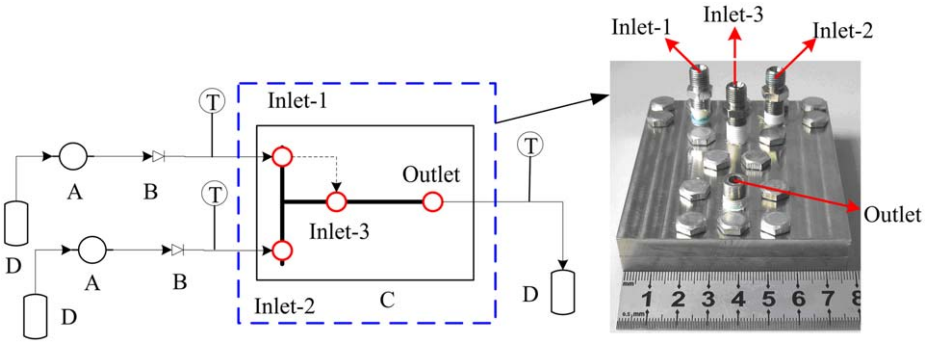

Fig. 2. Schematic diagram of experimental setup: (A) piston pump; (B) check valve; (C) T-junction microchannel; (D) separator.

The mass transfer coefficients are defined as follows:

$$ka \cdot t_i = \frac{q}{m+q} \ln \frac{C^*_{or,i} - C_{or,i}}{C^*_{or,i+1} - C_{or,i+1}} (i = 1,2,3,4) \quad (7)$$

The concentration profile is discontinuous at the interface of oil and water according to the equilibrium relationship:

$$C^*_{or,i} = mC_{aq,i} (i = 1,2,3,4,5) \quad (8)$$

The mass balance equation:

$$Q_{or} \cdot C_{or,i} + Q_{aq} \cdot C_{aq,i} = Q_{or} \cdot C_{or,i+1} + Q_{aq} \cdot C_{aq,i+1} (i = 1,2,3,4) \quad (9)$$

where the superficial residence time of the organic phase in the T-shaped microchannel system can be calculated by the following equation:

$$t_i = \frac{V_i}{Q_{or}} (i = 1,2,3,4) \quad (10)$$

$$t = t_1 + t_2 \quad (11)$$

2.5. Surface modification

In the present paper, the characteristics of flow patterns and mass transfer of liquid–liquid immiscible two phases are carried out in PMMA and stainless steel microchannels, respectively. Moreover, it has been confirmed that liquid–liquid two-phase flow patterns in microchannels are more seriously affected by the wettability between the wall and the fluids (Eggers, 1997; Squires and Quake, 2005). The contact angles of water and kerosene on PMMA material before surface modification are 76° and 8°, respectively. To increase the surface wettability, the PMMA chip is firstly immerged into the solution of sodium hydroxide, and finally its surface is coated by the alumina hydroxide sol. The contact angles of water and *n*-butanol on stainless steel material before surface modification are 54° and 0°, respectively. To increase the surface wettability of stainless steel chip, we coat the channel walls by physisorption silicon sol to change the surface properties of the stainless steel. The silicon dioxide coating increases (or decreases) the contact angle of *n*-butanol (water) and the channels wall, these changes can control the liquid–liquid two-phase flow patterns. The contact angles of water and *n*-butanol on stainless steel material after surface modification are 0° and 17.5°, respectively. Furthermore, the silicon sol coating method is simple and the coating can be selectively deposited on different sections of the microchannel using laminar flow of silicon sol. So the flow characteristics in different material microchannels can be linked up through surface modification of channel materials in the same operating conditions.

3. Results and discussions

3.1. Flow patterns before surface modification

Depending on the volume fraction of input organic phase (*n*-butanol), the mixture Reynolds numbers, the dimensions of microchannel and surface wettability of microchannel material, different liquid–liquid flow patterns can be encountered. Fig. 4 shows the effects of the mean Reynolds numbers on flow patterns of liquid–liquid immiscible two phases at the opposed T-junction and the fully developed flow zone before surface modification, respectively.

When two immiscible liquids are introduced to the opposed T-junction, the flow patterns are determined by the competing of interfacial tension and inertial force. At low flow rates, the interfacial tension dominates the inertia force, moreover, the organic phase has smaller contact angle than the aqueous phase on the PMMA material microchannel and the volumetric flux ratio ($q = Q_w/Q_o$) is greatly < 1, so the dispersed phase flow pattern that includes slug flow, monodispersed droplets can form. These

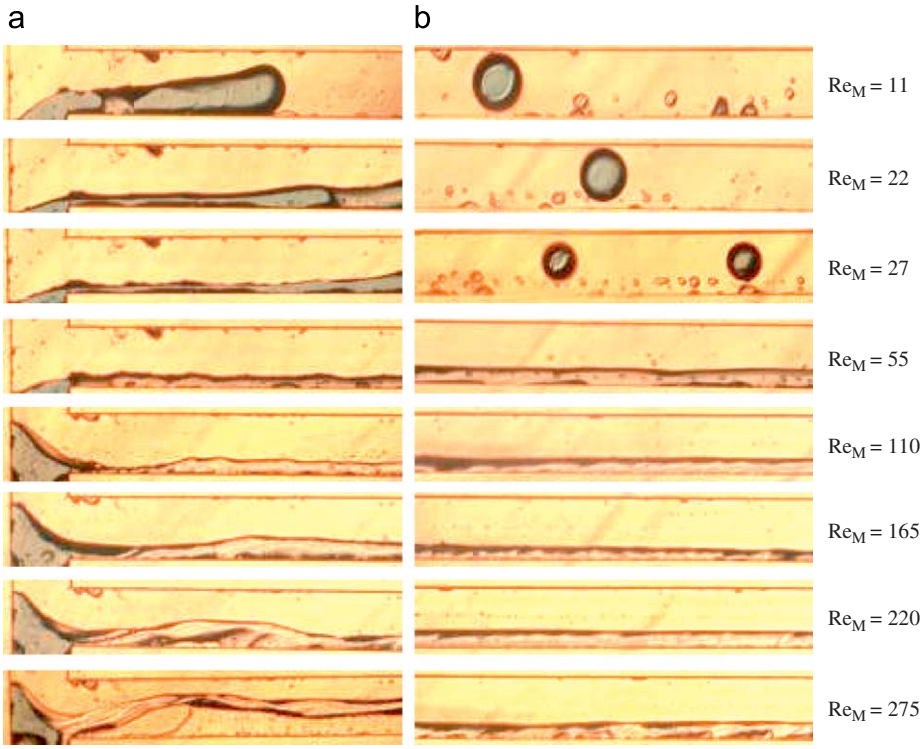

$q = 0.1$, $W = 600$ μm, $H = 300$ μm

Fig. 4. Flow patterns at the opposed T-junction (A) and in fully developed flow zone (B) before surface modification.

aqueous phase droplets are formed by interfacial instability which is induced through axial pressure gradient and interfacial tension.

For given fixed the volumetric flux ratio, the formation locations of water droplets gradually move to downstream due to an increase in the flow rates of two phases, and the volume of water droplets are reduced at the same time. Eventually, the parallel flow patterns are formed with the continual increase of the flow rate of two phases. The inertia force effects begin to play a significant role in forming water droplets with the increase of Re_M (the flow rate of two phases) numbers, the dispersed droplets are gradually difficult to form and replaced by parallel flow patterns ultimately. The experimental results show that the fluctuation (interface wave) in the interface of the two phases at the opposed T-junction and in fully developed flow zone cannot be observed at low Re_M numbers. When Re_M numbers are increased to above a threshold value, the interface wave which is induced by the unstability of Kelvin–Helmholtz (Funada and Joseph, 2001) occurs. The fluctuation amplitude increases with the increase of the flow rates of two phases; however, the wavelength shows the trend of decreasing. The fluctuation at the interface of the two phases can result in an increase on the interfacial area and the surface renewal velocity which significantly intensify mass transfer process and increase the overall volumetric mean mass transfer coefficient (Zhao et al., 2007).

3.2. Flow patterns after surface modification

The contact angle of aqueous phase on PMMA material microchannel can close to 0° after surface modification, therefore, the aqueous phase is preferential to be wetted compared to the organic phase. Fig. 5 shows the effects of the mixture Reynolds numbers on flow patterns of liquid–liquid immiscible two phases at the opposed T-junction and the fully developed flow zone after surface modification, respectively.

As can be observed in Fig. 5, only the continuous flow pattern (parallel flow pattern) can be formed after surface modification. The interface wave is quite stable at low Re_M numbers and shows instability at high Re_M numbers, moreover, the fluctuation amplitude increases with the increase of Re_M numbers. At the opposed T-junction, the amplitude is larger in comparison with the flow characteristics before surface modification. The weakening of the wettability performance of kerosene on microchannel wall after surface modification can result in the reducing of viscous dissipation and the increase of kinetic energy of organic phase in the opposed T-junction, so the intensity of the impinging of two immiscible fluids at the opposed T-junction is greatly enhanced, as can be shown in Figs. 4 and 5.

3.3. The effects of flow patterns on mass transfer in opposed configuration microchannel

As stated above, the flow characteristics of two immiscible fluids in the opposed T-shaped configuration microchannel are highly dependent on the surface properties of microchannel materials and Re_M numbers. In this section, the mass transfer characteristics in the opposed T-shaped configuration microchannel will be investigated. Figs. 6 and 7 show the effects of flow patterns at different volumetric flux ratios on the overall volumetric mean mass transfer coefficients (ka). It appears that the value of ka is found to increase with the increase of Re_M numbers, moreover, the threshold value (Re_M=60) for mass transfer performance is observed before and after surface modification in our experiments. The values of the overall volumetric mean mass transfer coefficient range from 0.27 to

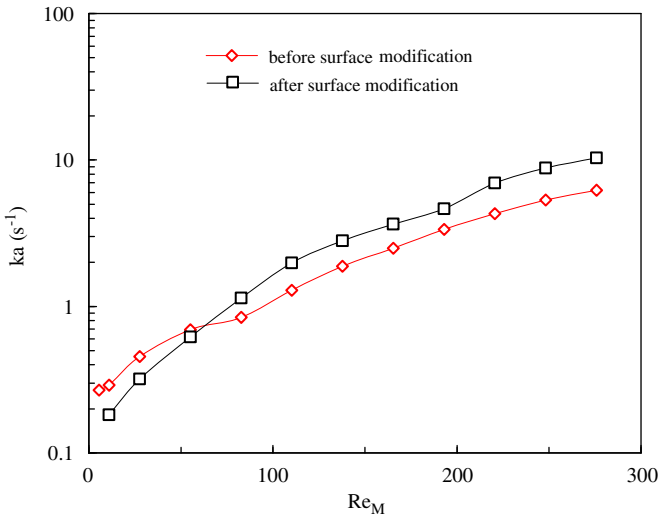

L = 60 mm, W = 600 μm, H = 300 μm, q = 0.1

Fig. 6. Effects of flow patterns on the overall volumetric mean mass transfer coefficient in the opposed T-junction microchannel.

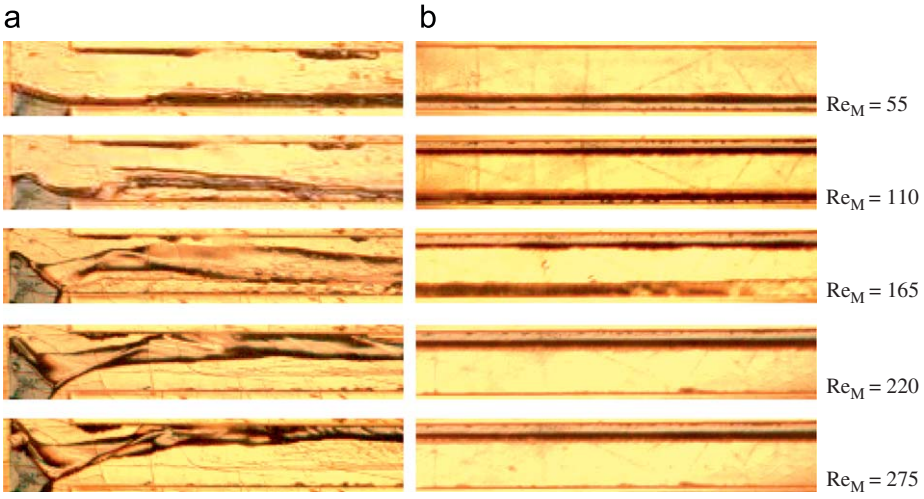

q = 0.1, W = 600 μm, H = 300 μm

Fig. 5. Flow patterns at the T-junction (A) and in fully developed flow zone (B) after surface modification.

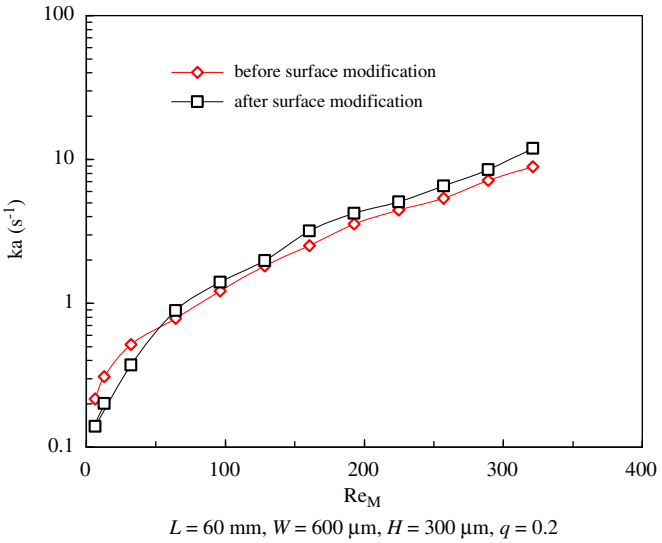

Fig. 7. Effects of flow patterns on the overall volumetric mean mass transfer coefficient in the opposed T-junction microchannel.

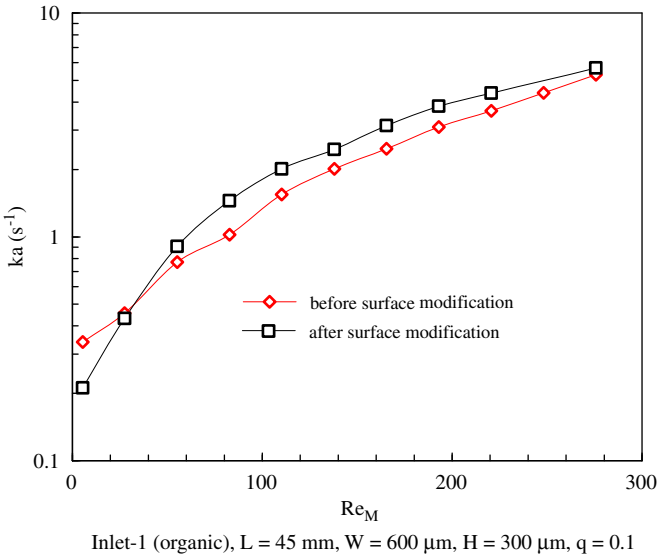

Fig. 8. Effects of flow patterns on *ka* in the cross-flow configuration microchannel.

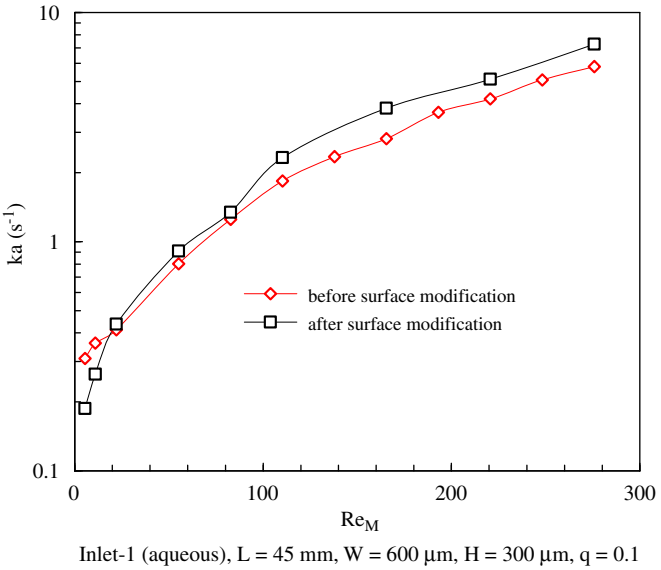

Fig. 9. Effects of flow patterns on *ka* in the cross-flow configuration microchannel.

8.93 s^{-1} before surface modification and from 0.19 to 11.96 s^{-1} after surface modification, respectively.

The overall volumetric mean mass transfer coefficients in the opposed T-shaped microchannel before surface modification are higher compared to after surface modification when Re_M numbers are lower than 60, as shown in Figs. 6 and 7. From our above experimental results we know that the microchannel walls are preferentially wetted by the organic phase before surface modification, so the dispersed water droplets can be easily formed under these conditions. Due to the internal circulation within the aqueous phase droplets, the boundary layer thickness is greatly reduced and limited to a region very close to the interface of two immiscible fluids. In addition, the surface renewal velocity of solute can be also increased. After surface modification, the contact angle of water on stainless steel is decreased to 0° and the microchannel walls are preferentially wetted by the aqueous phase, and so only the parallel flow pattern can be formed under these operating conditions. From our previous work (Zhao et al., 2007) we know that the intensification of the fluctuation in the interface of two phases on mass transfer is very weak or even can be ignored at lower Re_M numbers and mass transfer mainly depends on interface diffusion, therefore, the mass transfer performance is higher within the dispersed phase flow pattern zone compared to the continuous phase flow pattern.

From Figs. 6 and 7, we can see that the values of *ka* in the opposed T-shaped microchannel after surface modification are higher than before surface modification at higher Re_M numbers ($Re_M > 60$). The Kelvin–Helmholtz instability can cause the interface between two immiscible fluids that move at different velocities to form waves, and the mass transfer performance can be intensified through the instable interface wave. To the same operating conditions, the fluctuation amplitude after surface modification is larger than before surface modification at the opposed T-junction, as shown in Figs. 4 and 5. This may be explained the overall volumetric mean mass transfer coefficients before surface modification are lower than after surface modification.

3.4. The effects of flow patterns on mass transfer in cross-flow configuration microchannel

The effects of flow patterns on the overall volumetric mean mass transfer coefficients before and after surface modification are conducted at different Re_M numbers and some of the results are shown in Figs. 8 and 9. In Fig. 8, the organic and aqueous phases are introduced from inlet-1 and inlet-3, respectively. In Fig. 9, the organic and aqueous phases are introduced from inlet-3 and inlet-1, respectively. The overall volumetric mean mass transfer coefficients increase with the increase of Re_M numbers at different fluid inlet locations in cross-flow configuration microchannel, moreover, the threshold value (Re_M=30) for mass transfer performance is observed before and after surface modification in our experiments. From Figs. 6–9 we can see that the value of *ka* in the cross-flow configuration microchannel is lower at the same of Re_M numbers compared to the case of the opposed T-junction microchannel. This can be attributed to the different flow patterns in the opposed and the cross-flow configuration T-shaped microchannel and is in accordance with our previous experimental results (Zhao et al., 2007).

From Figs. 8 and 9, the values of *ka* in the cross-flow configuration microchannel after surface modification are lower

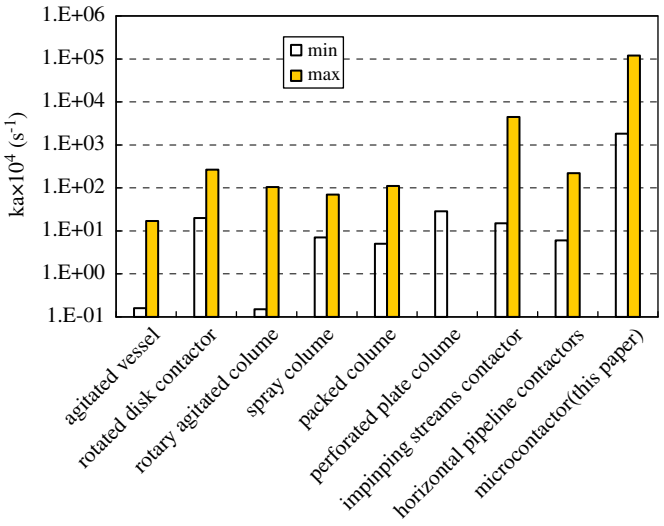

Fig. 10. Comparison of the liquid–liquid contactors.

than before surface modification at lower Re_M numbers ($Re_M < 30$), that is, the mass transfer performance of the dispersed phase flow pattern is better than the continuous phase flow pattern. With the increase of Re_M numbers, the dispersed phase flow pattern is gradually transformed into the continuous phase flow pattern and the fluctuation amplitude is enhanced simultaneously. When Re_M numbers are increased to above a threshold value (Re_M=30), the dispersed phase flow pattern becomes the continuous phase flow pattern and the overall volumetric mean mass transfer coefficients after surface modification are higher than before surface modification. This is attributed to the different surface properties before and after surface modification, as discussed in Section 3.3.

3.5. Comparison with conventional contactors

Based on the overall volumetric mean mass transfer coefficients, the microstructured contactors are compared with other conventional liquid–liquid contactors in Fig. 10, where the overall volumetric mean mass transfer coefficients are taken from pictures or tables presented in literatures (Laddha and Degaleesan, 1976; Shah and Sharma, 1971; Dehkordi, 2001) and from Figs. 6–9 in this paper, respectively.

From Fig. 10 we can see that the overall volumetric mass transfer coefficients obtained in the present investigation are more than one or three orders of magnitude higher than those typical conventional large scaled contactors. Therefore, the volume of microchannel mass transfer system can be greatly reduced compared to the conventional contactors when the same mass transfer process is accomplished.

4. Conclusions

The influence of surface properties on the flow characteristics and mass transfer performance of two immiscible liquids are investigated in the opposed and cross-flow T-shaped configuration microchannels, as the volumetric flux ratio is much <1. At low Re_M numbers, the dispersed phase flow pattern occurs in the opposed T-shaped PMMA microchannel before surface modification. At higher Re_M numbers, only the continuous phase flow pattern (parallel flow) is observed before and after surface modification. Moreover, the fluctuation amplitude after surface modification is larger than before surface modification at the opposed T-junction.

To eliminate the effects of the sampling intervals, one new testing method is established by manufacturing the novel oil–water separator based on the principle of siphon. For the conditions applied during the study, the overall volumetric mean mass transfer coefficients range from 0.19 to 11.96 s^{-1}, which are one or three orders of magnitude higher than those typical conventional large scaled contactors.

Notation

a	interfacial area, m^2/m^3
A	cross-sectional area of microchannel, m^2
$C_{aq,i}$	concentration of the solute of the inlet aqueous phase in i mass transfer zone, kg/m^3
$C_{or,i}$	concentration of the solute of the inlet organic phase at i mass transfer zone, kg/m^3
$C^*_{or,i}$	equilibrium concentration of the solute of the inlet organic phase in i mass transfer zone corresponding to the actual inlet concentration of the solute in the aqueous phase, kg/m^3
d	diameter of the side microchannel, m
D_H	hydraulic diameter of microchannel, m
h	microchannel height, m
k	overall mean mass transfer coefficient, m/s
ka	overall volumetric mean mass transfer coefficient, 1/s
L	channel length, m
m	partition coefficient of solute between aqueous and organic phases
$q = Q_{aq}/Q_{or}$	volumetric flux ratio
Re_M	mixture Reynolds number of the immiscible liquid–liquid two phases
t_i	superficial residence time of the aqueous phase in i mass transfer zone, s
U_M	mixture velocities of the immiscible liquid–liquid two phases, m/s
V_i	volume of i mass transfer zone, m^3
w	microchannel width, m

Greek letters

μ	viscosity, $Pa \cdot s$
ρ	mass density, kg/m^3
φ	hold-up fraction

Subscripts

aq	aqueous phase
i	location of the microchannel system
M	mixture of the immiscible liquid–liquid two phases
or	organic phase
1	at the T-junction zone
2	in the mixing channel zone
3	at the outlet conduit zone
4	during the falling droplets process zone
5	during the sampling in the phase separator zone

Acknowledgments

We gratefully acknowledge the financial supports for this project from Ministry of Science and Technology of China

(2009CB219903 and 2007AA030206) and National Natural Science Foundation of China (20676129).

References

Burns, J.R., Ramshaw, C., 2001. The intensification of rapid reactions in multiphase systems using slug flow in capillaries. Lab on a Chip 1, 10–15.

Burns, J.R., Ramshaw, C., 2002. A microreactor for the nitration of benzene and toluene. Chemical Engineering Communications 189, 1611–1628.

Cao, W.Q., Chen, G.W., Li, S.L., Yuan, Q., 2006. Methanol-steam reforming over a $ZnO–Cr_2O_3/CeO_2–ZrO_2/Al_2O_3$ catalyst. Chemical Engineering Journal 119, 93–98.

Chen, G.W., Yuan, Q., Li, H.Q., Li, S.L., 2004. CO selective oxidation in a microchannel reactor for PEM fuel cell. Chemical Engineering Journal 101, 101–106.

Dehkordi, A.M., 2001. Novel type of impinging streams contactor for liquid–liquid extraction. Industrial and Engineering Chemistry Research 40, 681–688.

Dessimoz, A.-L., Cavin, L., Renken, A., Kiwi-Minsker, L., 2008. Liquid–liquid two-phase flow patterns and mass transfer characteristics in rectangular glass microreactors. Chemical Engineering Science 63, 4035–4044.

Dreyfus, R., Tabeling, P., Willaime, H., 2003. Ordered and disordered patterns in two-phase flows in microchannels. Physical Review Letters 90, 144505.

Dummann, G., Quittmenn, U., Gröschel, L., Agar, D.W., Wörz, O., Morgenschweis, K., 2003. The capillary-microreactor: a new reactor concept for the intensification of heat and mass transfer in liquid–liquid reactions. Catalysis Today 79–80, 433–439.

Eggers, J., 1997. Nonlinear dynamics and breakup of free-surface flows. Reviews of Modern Physics 69, 865–929.

Ehrfeld, W., Hessel, V., Löwe, H., 2000. State of the art of microreaction technology. In: Microreactor: New Technology for Modern Chemistry. Wiley, Weinheim.

Funada, T., Joseph, D.D., 2001. Viscous potential flow analysis of Kelvin–Helmholtz instability in a channel. Journal of Fluid Mechanics 445, 263–283.

Guillot, P., Colin, A., 2005. Stability of parallel flows in a microchannel after a T junction. Physical Review E 72, 066301.

Hu, J.L., Wang, Y., Cao, C.S., Elliott, D.C., Stevens, D.J., White, J.F., 2005. Conversion of biomass syngas to DMF using a microchannel reactor. Industrial and Engineering Chemistry Research 44, 1722–1727.

Jähnisch, K., Hessel, V., Löwe, H., Baerns, M., 2004. Chemistry in microstructured reactors. Angewandte Chemie International Edition 43, 406–446.

Jensen, K.F., 2001. Chemical Engineering Science 56, 293–303.

Kashid, M.N., Harshe, Y.M., Agar, D.W., 2007. Liquid–liquid slug flow in a capillary: an alternative to suspended drop or film contactors. Industrial and Engineering Chemistry Research 46, 8420–8430.

Kashid, M.N., Gerlach, I., Goetz, S., Franzke, J., Acker, J.F., Platte, F., Agar, D.W., Turek, S., 2005. Internal circulation within the liquid slugs of a liquid–liquid slug-flow capillary microreactor. Industrial and Engineering Chemistry Research 44, 5003–5010.

Kockmann, N., 2007. Transport Phenomena in Microprocess Engineering. Springer.

Laddha, G.S., Degaleesan, T.E., 1976. Transport Phenomena in Liquid Extraction. McGraw-Hill, New Delhi, India.

Mala, G.M., Li, D.Q., Dale, J.D., 1997. Heat transfer and fluid flow in microchannels. International Journal of Heat and Mass Transfer 40, 3079–3088.

Misek, T., Berger, R., Schröter, J., 1985. Standard Test Systems for Liquid Extraction, second ed., European Federation of Chemical Engineering, EFCE Publications Series No. 46.

Shah, A.K., Sharma, M.M., 1971. Mass transfer in liquid–liquid (horizontal) pipeline contactors. The Canadian Journal of Chemical Engineering 49, 596–604.

Squires, T.M., Quake, S.R., 2005. Microfluidic: fluid physics at the nanoliter scale. Reviews of Modern Physics 77, 977–1026.

Thorsen, T., Roberts, R.W., Arnold, F.H., Quake, S.R., 2001. Dynamic pattern formation in a vesicle-generating microfluidic device. Physical Review Letters 86, 4163–4166.

Tunc, G., Bayazitoglu, Y., 2002. Heat transfer in rectangular microchannels. International Journal of Heat and Mass Transfer 45, 765–773.

van der Linden, H.J., Jellema, L.C., Holwerda, M., Verpoorte, E., 2006. Stabilization of two-phase octanol/water flows inside poly(dimethylsiloxane) microchannels using polymer coatings. Analytical and Bioanalytical Chemistry 385, 1375–1383.

Zhao, B., Moore, J.S., Beebe, D.J., 2002. Principles of surface-directed liquid flow in microfluidic channels. Analytical Chemistry 74, 4259–4268.

Zhao, Y.C., Chen, G.W., Yuan, Q., 2006. Liquid–liquid two-phase flow patterns in a rectangular microchannel. A.I.Ch.E. Journal 52, 4052–4060.

Zhao, Y.C., Chen, G.W., Yuan, Q., 2007. Liquid–liquid two-phase mass transfer in the T-junction microchannels. A.I.Ch.E. Journal 53, 3042–3053.